Arf tumor suppressor promoter monitors latent oncogenic signals *in vivo*

Frederique Zindy*, Richard T. Williams†, Troy A. Baudino‡, Jerold E. Rehg§, Stephen X. Skapek†, John L. Cleveland‡, Martine F. Roussel*, and Charles J. Sherr*¶‖

Departments of *Genetics and Tumor Cell Biology, †Hematology–Oncology, ‡Biochemistry, and §Pathology and ¶Howard Hughes Medical Institute, St. Jude Children's Research Hospital, 332 North Lauderdale Street, Memphis, TN 38105

Contributed by Charles J. Sherr, October 21, 2003

Induction of the *Arf* tumor suppressor gene by elevated thresholds of mitogenic signals activates a p53-dependent transcriptional response that triggers either growth arrest or apoptosis, thereby countering abnormal cell proliferation. Conversely, *Arf* inactivation is associated with tumor development. Expression of *Arf* in tissues of adult mice is difficult to detect, possibly because its induction leads to the arrest or elimination of incipient tumor cells. We replaced coding sequences of exon 1β of the mouse cellular *Arf* gene with a cDNA encoding GFP, thereby producing *Arf*-null animals in which GFP expression is driven by the intact *Arf* promoter. The *Arf* promoter was induced in several biologic settings previously shown to elicit mouse p19^{Arf} expression. Inactivation of *Arf* in this manner led to the outgrowth of tumor cells expressing GFP, thereby providing direct evidence that the *Arf* promoter monitors latent oncogenic signals *in vivo*.

The *Ink4a-Arf* locus encodes two tumor suppressor proteins, p16^{Ink4a} and p19^{Arf}, that up-regulate the activities of the retinoblastoma protein (Rb) and the p53 transcription factor, respectively (1). The p16^{Ink4a} protein inhibits the activity of cyclin D-dependent kinases, thereby maintaining Rb in its hypophosphorylated, growth-suppressive state, whereas p19^{Arf} antagonizes Mdm2 activity to induce a p53 transcriptional response that leads to cell cycle arrest or apoptosis, depending on the biologic setting. Targeted disruption of *Ink4a*, *Arf*, or both genes in the mouse strongly predisposes them to tumor development (2–5); similarly, their inactivation by mutation, deletion, or epigenetic silencing is observed in many human cancers (6, 7).

The *Ink4a-Arf* locus is unusual because the transcripts of two alternative first exons are spliced to that of a shared second exon, whose sequences are translated in two different reading frames (8). However, despite this economical gene structure, the separate *Ink4a* and *Arf* promoters can differentially respond to input signals and be independently silenced in tumors. *Arf* is not usually expressed in normal tissues but is induced by sustained and elevated mitogenic signals that may stem from oncogene activation (1). For example, whereas physiologic thresholds of Myc and Ras signaling do not activate *Arf* gene expression, overexpression of *Myc* (9) and sustained signaling by oncogenic *Ras* (10) induce *Arf* to trigger p53 activity. This process counters aberrant mitogenic signaling by inducing growth arrest or apoptosis in cells that might otherwise give rise to tumors. Metaphorically, then, *Arf* acts as a fuse that monitors mitogenic current and is activated when signaling circuits are overloaded. Understanding how the *Arf* promoter distinguishes between normal and abnormal signaling thresholds remains a challenging problem (1).

Although much of p19^{Arf}'s activity depends on p53, inactivation of *Arf* in mice lacking both *Mdm2* and *p53* leads to a much more rapid appearance of tumors than that observed in animals lacking any one or two of these genes (11). Tumors spontaneously appear even before these triple knockout animals reach reproductive age, and multiple tumors routinely arise from different tissue types in individual animals. Moreover, introduction of *Arf* into cells lacking *p53*, or both *Mdm2* and *p53*, can arrest proliferation, albeit much less efficiently than in cells that retain Mdm2 and p53 function (11, 12). Therefore, p19^{Arf}, Mdm2, and p53 cannot function in a strictly linear signaling pathway, and p19^{Arf} has activities that do not depend on Mdm2 and p53. At least some of the p53-independent effects of p19^{Arf} might be mediated by its ability to inhibit ribosomal RNA processing (13) and to indirectly induce genes regulating other antiproliferative and apoptotic programs (14, 15).

It is unlikely that the normal physiologic role of *Arf* is to guard against tumorigenesis, particularly in short-lived species, such as mice, that rarely develop cancers spontaneously. To date, the only context in which *Arf* loss has been found to affect normal development is in the eyes of newborn mice, where excess retrolental tissue and persistence of the hyaloid vasculature in the vitreous result in destruction of both the lens and neuroretina (16). To ultimately discern how the *Arf* gene is regulated *in vivo*, we replaced *Arf* exon 1β coding sequences with a cassette specifying GFP, thereby disabling *Arf* function and placing *GFP* under the control of the cellular *Arf* promoter. Although most normal tissues of *Arf* $^{GFP/GFP}$ mice expressed negligible GFP levels, tumors and ocular masses exhibited vivid green fluorescence, indicating that the *Arf* promoter responds to aberrant signals in these pathologic settings.

Materials and Methods

Targeting Vector. A 1-kb *Sma*I fragment containing exon 1β (Fig. 1) was altered by using PCR-based primers to create a site of restriction for *Nco*I at the *Arf* ATG codon and an *Xho*I site 16 nucleotides 5′ to the 3′ splice donor site. An *Nco*I–*Hin*dIII restriction fragment containing cDNA specifying enhanced GFP and a 3′ polyadenylation signal (Clontech) was ligated in orientation opposite to a neomycin resistance (*neo*) gene flanked by its own 5′ promoter and 3′ polyadenylation signal (Stratagene) to create an *Nco*I–*Xho*I fragment that was substituted for coding sequences in *Arf* exon 1β. This substitution left intact the *Arf* promoter and 5′ untranslated sequences and recreated the ATG codon to enable GFP translation. Sequences encoding the exon 1β splice donor site were retained 3′ of the *neo* gene but are prevented from being transcribed by the *GFP* polyadenylation signal. A cassette encoding the diphtheria toxin A-chain (DT-A) was appended to the 5′ end of the vector to allow selection against nonhomologous recombination elsewhere in the mouse genome (17).

Homologous Recombination and Generation of Knock-in Mice. W9.5 129/SvJ embryonic stem (ES) cells were electroporated with the linearized targeting vector and selected with G418 (Gibco Invitrogen) as described (3). DNAs from 490 drug-resistant colonies were screened by Southern blotting after restriction with *Afl*II and hybridization with a unique sequence *Spe*I–*Cla*I

Abbreviations: MEF, mouse embryo fibroblast; ES, embryonic stem.

‖To whom correspondence should be addressed. E-mail: sherr@stjude.org.

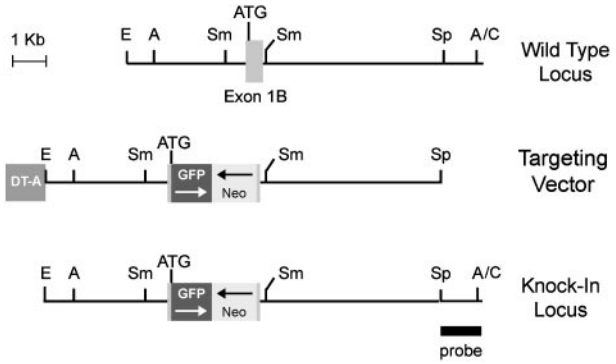

Fig. 1. Targeting of the *Arf* locus surrounding exon 1β. A schematic map of the region flanking exon 1β (*Top*), relevant sequences in the targeting vector (*Middle*), and the knock-in allele (*Bottom*) are illustrated. *Arf* coding sequences were replaced by a cassette encoding enhanced GFP and the neomycin-resistance gene (*neo*) in opposite orientations (arrows). The *neo* gene includes its own 5′ promoter, whereas GFP expression is driven by the *Arf* promoter; both *neo* and *GFP* terminate with 3′ polyadenylation signals. The targeting vector contains a gene encoding the diphtheria toxin A chain (DT-A), which is toxic unless eliminated and therefore selects against nonhomologous recombination of the targeting vector elsewhere in the mouse genome. The probe used to score the different alleles is illustrated at the bottom right. ATG refers to the position of the GFP initiation codon. Restriction sites for *EcoR1* (E), *Afl*II (A), *Sma*I (Sm), *Spe*I (Sp), and *Cla*I (C) are indicated.

probe (Fig. 1 *Bottom*). Three ES clones exhibiting correct homologous recombination and normal karyotypes were injected into C57BL/6 blastocysts, which were implanted into the uteri of pseudopregnant B6CBA F_1/J foster mothers and allowed to develop to term. Male chimeras derived from the three ES clones were mated to C57BL/6 females that transmitted the knock-in allele through the germ line. As anticipated (3), heterozygous offspring gave rise to normally developing animals that segregated the knock-in allele at the expected Mendelian frequency. F_1 animals were interbred to generate F_2 littermates used in subsequent studies. The three *Arf-GFP* strains were phenotypically identical.

Mouse Maintenance, Interbreeding, and Imaging. Where indicated, cohorts of *Arf* $^{GFP/GFP}$ animals received single 4-Gy exposures of ionizing radiation 5 days after birth or were left untreated and monitored for tumor development. *Arf*$^{GFP/GFP}$ mice were bred to Eμ-*Myc* C57BL/6 transgenic mice to generate *Arf*$^{+/GFP}$ F_1 offspring expressing the *Myc* transgene. Animals were examined at least twice weekly for signs of disease. Mice were maintained and humanely killed when moribund in accordance with Institutional Animal Care and Use Committee guidelines. Tumors were harvested immediately and were snap-frozen in liquid nitrogen. Survival curves were calculated as described (18).

Animals were examined by total-body fluorescence imaging (19, 20) during the course of tumor development. Selective excitation of GFP was produced by using an Illumatool TLS system with an excitation band-pass filter at 470 nm, and emitted fluorescence was collected through a long-pass filter at 515 nm (Lightools Research, Encinitas, CA) on a three-chip cooled color charge-coupled device camera (C5810, Hamamatsu Photonics Systems, Hamamatsu City, Japan). IMAGE PRO PLUS 4.5.1 software (Media Cybernetics, Silver Spring, MD) was used to analyze digital images of 1,024 $\times$ 724 pixels captured directly on a computer equipped with a high-resolution light-emitting diode screen.

Flow Cytometry. Bone marrow, spleen, and lymph node cells were harvested from precancerous and lymphomatous mice and red blood cells were lysed in hypotonic buffer (18). Cells collected by low-speed centrifugation were suspended at 1×10^6 per 0.1 ml and incubated for 30 min on ice in 2% FBS in PBS containing a 1:200 dilution of photofluor-conjugated antibody to B220 (RA3-6B2, BD Biosciences Pharmingen). Cells were washed, resuspended in staining buffer, and analyzed by flow cytometry for GFP (excitation at 488 nm; emission at 519 nm) and for B220 binding (excitation at 633 nm; emission at 660 nm).

Mouse Embryo Fibroblast (MEF) Cultures and Viral Transduction. MEFs from midgestation embryos were explanted and propagated as described (3). pBABE retroviral vectors expressing either a puromycin-resistance gene (*puro*) alone or both *puro* and oncogenic Harvey *Ras* (21) (a gift from S. Lowe, Cold Spring Harbor Laboratory, Cold Spring Harbor, NY) were packaged by using ecotropic helper virus in human kidney 293T cells and used to infect MEFs (9). Primary MEFs at passages 2–5 were plated under sparse conditions (2×10^5 cells per 100-mm-diameter culture dish) on day -1, infected on day 0 with retroviruses, and selected for 2 days after infection with 2 μg/ml puromycin. Cultures were harvested on days 3 and 4 after infection. Cells diluted to the original concentration and replated on day 4 were harvested 3 days later (day 7). Cells were assayed by flow cytometry for GFP fluorescence and by immunoblotting for GFP protein (Ab7.1 and 13.1, 0.4 μg/ml, Roche Diagnostics) and $p19^{Arf}$ expression (0.5 μg/ml Ab80, AbCam, Cambridge, MA) (9).

Tumor Pathology and GFP Staining. Formalin-fixed, paraffin-embedded tumor specimens were sectioned at 5 μm, stained with hematoxylin and eosin, and examined by light microscopy. Immunocytochemistry for various discriminating markers was performed as described in detail (22, 23). Partially dissected eyes from newborn mice were studied by light and fluorescence microscopy. Detection of GFP was performed with 12-μm frozen sections of testis fixed in 4% paraformaldehyde in PBS. Sections were incubated for 30 min at room temperature in PBS containing 0.1% Triton X-100 and 10% goat serum followed by overnight incubation at 4°C with rabbit polyclonal anti-GFP (1:1,000; Molecular Probes) and 1-h incubation at room temperature with cy-3-conjugated goat anti-rabbit IgG (1:200; Jackson ImmunoResearch). Antibodies were diluted in PBS containing 0.1% Triton X-100 and 2% goat serum. Stained tissues were mounted by using vectashield (Vector Laboratories) containing 4′,6-diamidino-2-phenylindole and imaged with a Zeiss 510 NLO multiphoton/confocal laser-scanning microscope. The multiphoton infrared laser was used to excite 4′,6-diamidino-2-phenylindole (blue), and the confocal HeNe laser was used to excite Cy3 (red).

Results

***Arf*$^{GFP/GFP}$ MEFs Express GFP in Response to "Culture Shock" and Oncogenic Ras.** With the exception of the yolk sac (L. Nilsson and F.Z., unpublished data) and postnatal eye (16), *Arf* is not detectably expressed during normal mouse development (24). However, MEFs derived from midgestation embryos and serially passaged in culture are induced to synthesize $p19^{Arf}$, which accumulates as the cells lose their proliferative capacity and eventually senesce (9). Conversely, MEFs lacking *Ink4a-Arf* (2) or *Arf* alone (3) do not senesce and readily emerge as immortalized cell lines sensitive to transformation by oncogenic *Ras*. Although *Arf* induction in primary MEFs normally accompanies the stress of *ex vivo* culture, the process is accelerated by oncogenic *Ras*, resulting in earlier senescence (25).

MEFs prepared from *Arf*$^{+/+}$, *Arf*$^{+/GFP}$, or *Arf*$^{GFP/GFP}$ embryos were infected with a control retroviral vector or one encoding oncogenic Ras. Cells plated in sparse cultures and allowed to proliferate began to express GFP, which accumulated during the first week of culture (Fig. 2 *A* and *B Bottom*). MEFs expressing

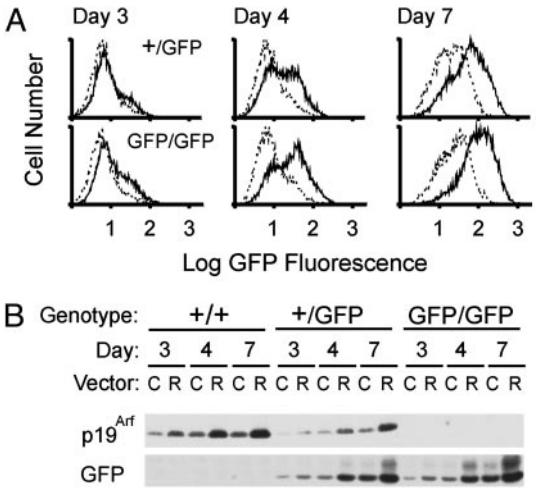

Fig. 2. Analysis of GFP and p19^{Arf} expression in MEFs. (*A*) *Arf*$^{+/GFP}$ (*Upper*) and *Arf*$^{GFP/GFP}$ (*Lower*) MEFs infected with a control retroviral vector (dotted lines) or a vector encoding oncogenic Ras (solid lines) were scored for green fluorescence by flow cytometry at the indicated times after plating in sparse culture. (*B*) Equal quantities of protein from detergent lysates of wild-type (+/+) MEFs and from the cells of the indicated genotypes analyzed in *A* were separated on denaturing gels, transferred to a membrane, and blotted with antibodies to p19^{Arf} or GFP as indicated at the bottom. Blotting with antibodies to actin served as an internal loading control (data not shown). Cells infected with the control vector (C) or the one encoding Ras (R) were analyzed at the same times after plating as those in *A*.

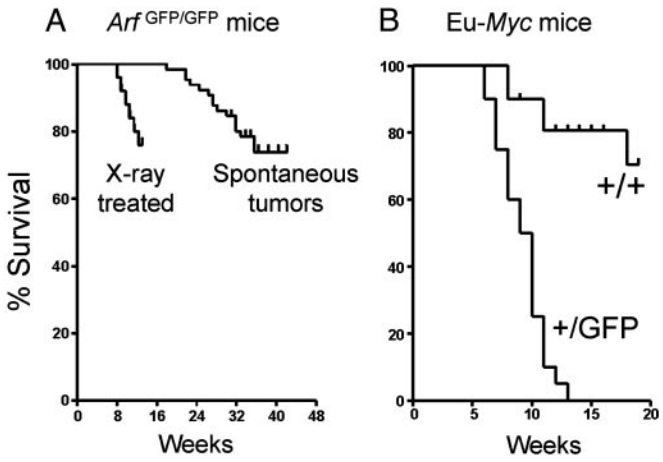

Fig. 3. Mouse survival curves. (*A*) Rates of spontaneous tumor development in *Arf* $^{GFP/GFP}$ mice observed for up to 44 weeks after birth, as compared with those arising in animals that received a single sublethal dose of ionizing irradiation at 5 days of age. (*B*) Rates of lymphoma development in Eμ-*Myc* transgenic mice contrasted on an *Arf*$^{+/+}$ or *Arf*$^{+/GFP}$ genetic background.

oncogenic *Ras* exhibited faster induction of GFP, whether they retained a copy of the wild-type *Arf* allele or not. *Arf*$^{+/+}$ and *Arf*$^{+/GFP}$ MEFs also expressed increasing levels of p19^{Arf} protein that accumulated more rapidly in cells expressing Ras (Fig. 2*B Top*). MEFs from *Arf*$^{+/GFP}$ mice expressed approximately half of the p19^{Arf} protein detected in matched Arf$^{+/+}$ controls and less GFP protein than *Arf*$^{GFP/GFP}$ MEFs. Thus, in cells from heterozygotes, the *GFP* knock-in allele had no discernable effect on expression of the wild-type *Arf* gene or vice versa. *Arf*$^{GFP/GFP}$ MEFs did not senesce and were maintained for as many as 20 passages as cell lines; these cells were sensitive to morphologic transformation by oncogenic Ras (data not shown), consistent with the idea that they are functionally *Arf*-null. As expected (3), p16^{Ink4a} was continuously expressed, as documented by immunoblotting (data not shown). Therefore, despite the lack of p19^{Arf} protein production and the failure of *Arf*$^{GFP/GFP}$ MEFs to undergo senescence, the *Arf* promoter appeared to properly regulate GFP expression.

***Arf*$^{GFP/GFP}$ Mice Are Prone to Tumor Development.** The majority of *Arf*-null mice develop tumors in their first year of life, and virtually all succumb to cancers in their second (3, 26). The most prevalent tumors are sarcomas and lymphomas, although carcinomas and gliomas are detected less frequently. Although *Arf* is not induced by ionizing radiation (3, 27), tumor development in *Arf*-null strains is accelerated in animals exposed neonatally to x-rays or chemical carcinogens (26).

Untreated *Arf*$^{GFP/GFP}$ mice also developed tumors, which arose more rapidly in animals that received a single 4-Gy dose of total body irradiation 5 days after birth (Fig. 3*A*). Histopathologic analysis of 26 mice that spontaneously developed tumors revealed a broad disease spectrum. Most (65% in this series) were highly invasive sarcomas of various types, including those with pleomorphic morphology (seven cases), gastrointestinal stromal tumors (three cases), hemangiosarcomas (three cases), malignant peripheral nerve sheath tumors (two cases), and histiocytic sarcomas (two cases). Lymphomas (33%) comprised the remainder. Although we analyzed a relatively small cohort of animals, the 2:1 frequency of sarcomas versus lymphomas mimics that seen in *Arf*-null mice (26).

Depending on tumor type, size, and anatomic location, many solid tumors exhibited vivid green fluorescence (Fig. 4 *A* and *B*). Spontaneously arising lymphomas that metastasized to liver sometimes appeared macroscopically as green fluorescent nod-

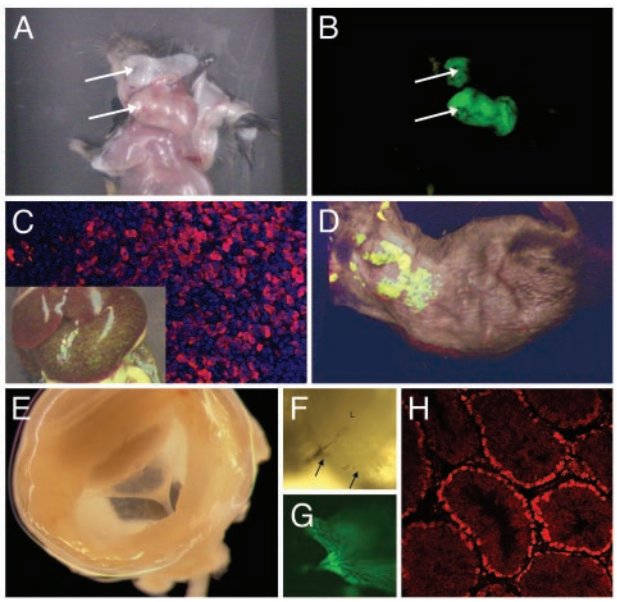

Fig. 4. GFP expression in mouse tissues. (*A* and *B*) *Arf* $^{GFP/GFP}$ mouse with a green fluorescent sarcoma (arrows) in the neck region. (*C*) Illustration of macroscopic foci of GFP-positive lymphoma cells that metastasized to liver (*Inset*) and microscopic foci visualized by immunofluorescence (red) and counterstained with 4′,6-diamidino-2-phenylindole (blue). (*D*) Whole-body imaging of a shaved *Arf* $^{+/GFP}$, Eμ-*Myc* mouse with lymphoma. A whole mount of a dissected eye from an *Arf*$^{GFP/GFP}$ mouse (*E*) illustrates a funnel-shaped mass stretching from the lens (top left) toward the optic cup at the rear. A closer view (*F*) illustrates elements of the hyaloid vasculature (arrows) within the green fluorescent mass (*G*). (*H*) Immunohistochemical staining of GFP (red) in the testis of an 8-month-old mouse. The position of stained cells within the tubules closely corresponds to regions containing spermatogonia and immature (leptotene) spermatocytes in meiosis I.

ules (Fig. 4*C Inset*). Even when metastatic foci were not visible by eye, immunohistochemical analysis and the use of a more sensitive two-photon confocal laser microscope demonstrated invasion of the liver parenchyma by GFP-positive lymphoma cells (Fig. 4*C*, GFP in red, 4′,6-diamidino-2-phenylindole in blue). Half of the mice had enlarged spleens with extensive foci of extramedullary hematopoiesis, a finding observed in animals lacking *Ink4a-Arf* or *Arf* alone (2, 3). Together, these results argue that although $Arf^{GFP/GFP}$ mice have lost *Arf* tumor suppressor activity, the retained *Arf* promoter continues to actively drive GFP expression in tumor cells.

***Myc* Activates the *Arf-GFP* Allele *in Vivo*.** When overexpressed, c-Myc is a potent *Arf* inducer, and its proapoptotic activities are mediated in part by its ability to trigger $p19^{Arf}$-dependent expression of p53 (9). Conversely, loss of either $p19^{Arf}$ or p53 function greatly dampens Myc's ability to kill cells and thereby allows overexpressed Myc to act as a more potent promoter of cell growth and proliferation. These effects can be readily appreciated in the Eμ-*Myc* mouse model of Burkitt's lymphoma, in which a *Myc* transgene driven by the Ig heavy-chain promoter-enhancer (Eμ) induces B cell tumors (28). Mice expressing the transgene routinely develop B cell lymphomas with a mean latency of ≈26 weeks, and all die of disease by 1 year after birth (Fig. 3*B*). When crossed with $Arf^{+/-}$ heterozygotes, disease latency is shortened to ≈12 weeks, and >80% of the lymphomas that arise lose the wild-type *Arf* allele, consistent with the idea that *Arf* functions as a prototypic "two-hit" tumor suppressor (18, 29, 30). Similar results were obtained in $Arf^{+/GFP}$ mice (Fig. 3*B*), except that the resulting lymphomas exhibited green fluorescence. Indeed, we have been able to observe disease development in real time in $Arf^{+/GFP}$ animals (Fig. 4*D*), as have others who used transplanted lymphoma cells that were engineered to express GFP (20, 31).

Lymphoid organs from precancerous Eμ-*Myc* transgenic mice exhibit a high proliferative index that is offset by apoptosis. Only later in the course of disease does inactivation of *p53* or *Arf* cancel apoptosis and result in the rapid expansion of *Myc*-expressing lymphoma cells (18). To determine whether we might be able to detect Myc-induced *Arf* promoter activity before the emergence of frank disease, we harvested splenocytes and bone marrow cells from young $Arf^{+/GFP}$ mice and simultaneously assayed B220-positive B cells for GFP expression. Neither spleen nor bone marrow cells from $Arf^{+/+}$, Eμ-*Myc* transgenic mice expressed GFP (Fig. 5 *A* and *B*), whereas a substantial fraction of B220-positive B cells from $Arf^{+/GFP}$, Eμ-*Myc* transgenic mice exhibited green fluorescence (Fig. 5 *C* and *D*). A much smaller fraction of B220-negative cells in the spleen expressed GFP (Fig. 5*C*); these cells are likely to be more mature B cells that are not present in the bone marrow (Fig. 5*D*) (18, 28). Spleen and bone marrow from nontransgenic $Arf^{+/GFP}$ animals did not express GFP (Fig. 5 *E* and *F*), in agreement with previous findings that Eμ-*Myc* is required to drive *Arf* expression in B cells. Splenocytes (Fig. 5*G*) and lymph node cells (Fig. 5*H*) taken from mice with overt lymphomas exhibited even greater degrees of GFP expression, and involved lymph nodes could be detected in living mice by using whole-body fluorescence imaging (Fig. 4*D*).

***Arf-GFP* Expression in the Vitreous of the Mouse Eye.** During the first week of postnatal development, *Arf* is induced in the vitreous of the eye where its expression is required for regression of the hyaloid vascular system that nourishes the developing lens and vitreous. In newborn *Arf*-null mice, the hyaloid vasculature persists and is associated with an abnormal proliferation of perivascular cells that form a funnel-shaped retrolental mass that ultimately disrupts the architecture of the posterior lens and the neuroretina (16).

Eye development in $Arf^{+/GFP}$ mice proceeds normally, although examination of the hyaloid vasculature at the time that *Arf* is normally expressed allowed us to visualize a few green fluorescent cells (data not shown). As expected, $Arf^{GFP/GFP}$ mice developed the characteristic pathologic findings previously observed in the *Arf*-null strain, except that the funnel-shaped retrolental mass in the vitreous included green fluorescent cells. Fig. 4*E* shows a whole mount of a dissected eye from a mouse at postnatal day 4 in which the vitreal mass was clearly visualized. A closer view illustrates vascular elements within the mass (Fig. 4*F*) surrounded by green fluorescent cells (Fig. 4*G*). These findings provide further compelling evidence that $Arf^{GFP/GFP}$ animals lack a functional *Arf* gene and that the intact *Arf* promoter responds appropriately to physiologic signals that normally promote vascular regression in the eye.

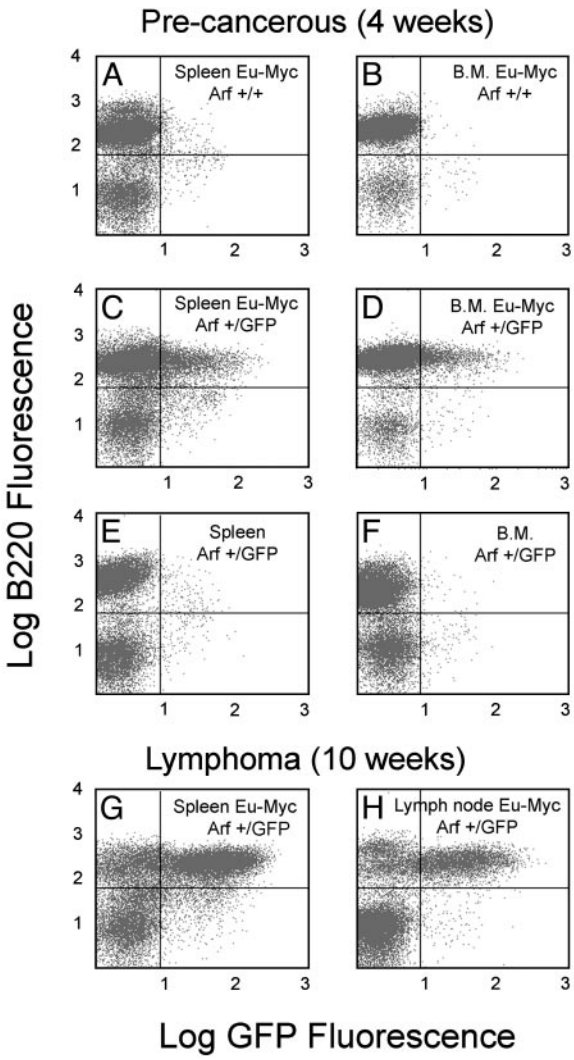

Fig. 5. Flow cytometric analysis of lymphoid cells expressing GFP. (*A–F*) Illustration of results obtained from 4-week-old mice that exhibited no overt signs of lymphoma development (precancerous). (*G* and *H*) Documentation of GFP expression in older lymphomatous animals. Results with splenocytes are shown in *A*, *C*, *E*, and *G*, results with bone marrow (B.M.) are shown in *B*, *D*, and *F*, and results with lymph node cells are shown in *H*. The genotypes of the mice are indicated in the upper right of each panel. Cells were costained for the B cell marker B220 (ordinate) or for GFP (abscissa) and analyzed by dual-color flow cytometry.

***Arf* Promoter Expression in the Testis.** A previous analysis of newborn mice indicated that the first detectable site of *Arf*

expression in otherwise normal tissue is in the testis (24). Because immunohistochemical identification of $p19^{Arf}$ protein has not so far been achieved, the cells that express $p19^{Arf}$ have not been identified. We prepared sections from the testis of male mice of various ages but were unable to detect GFP expression by fluorescence microscopy. However, immunohistochemical staining allowed ready detection of GFP expression in testicular tubules from adult $Arf^{GFP/GFP}$ mice (Fig. 4*H*). In sections taken from animals from 2 to 8 months of age, staining was limited to cells lining the tubules, which, based on their location and morphology, most likely represent either spermatogonia or leptotene spermatocytes at the earliest stages of meiosis I (32). Thus, the low levels of *Arf* expressed within the normal testis appear to be limited to cells that switch from a mitotic to a meiotic division cycle.

Using the same technique, we have visualized small pockets of green fluorescent cells in other ostensibly normal tissues, including the thymic medulla, lung alveoli, and regions of the brain and gastrointestinal tract (data not shown). We are now attempting to use other lineage-specific markers to identify the nature of the GFP-positive cells in young $Arf^{+/GFP}$ and $Arf^{GFP/GFP}$ mice. As yet, we have no clear idea of the identity of these cell populations, but our preliminary analysis indicates that such cells are rare and express only low levels of GFP, in agreement with earlier studies that *Arf* expression is difficult to detect in most normal tissues (24).

Discussion

The $Arf^{GFP/GFP}$ mouse strain lacks sequences encoding the $p19^{Arf}$ tumor suppressor protein and therefore exhibits phenotypic characteristics seemingly identical with those of *Arf*-null strains described (3–5). First, MEFs derived from these animals did not undergo senescence and were susceptible to transformation by oncogenic *Ras*. Second, $Arf^{GFP/GFP}$ mice spontaneously developed tumors, and these arose more rapidly when neonatal mice were exposed to a single sublethal dose of ionizing radiation. Third, lymphomagenesis induced by an Eμ-*Myc* transgene was greatly accelerated in the $Arf^{+/GFP}$ genetic background, in which the latency of disease was shortened from ≈26 to ≈12 weeks. As expected, the wild type *Arf* allele was lost from the vast majority of the tumors that arose (ref. 18 and data not shown), consistent with *Arf*'s behavior as a prototypic "two-hit" tumor suppressor in this model system. Finally, newborn $Arf^{GFP/GFP}$ mice exhibited ocular pathology due to the presence of bilateral retrolental masses associated with failure of hyaloid vasculature regression in the vitreous and destruction of the retina and the lens.

We found that GFP was expressed in all these biologic settings. Specifically, cultured MEFs, spontaneously arising tumors, Eμ-*Myc*-induced lymphomas, and retrolental masses in the vitreous of the eye each exhibited green fluorescence. Therefore, even in the complete absence of functional Arf protein, the *Arf-GFP* promoter-reporter responds *in vivo* to signals that would otherwise induce $p19^{Arf}$ expression. We reason that *Arf*-inductive signals arising in wild-type mice would normally lead to a p53 response that counters cell proliferation by cell cycle arrest or apoptosis, ultimately limiting the number of *Arf*-expressing cells. In contrast, *Arf* inactivation permits persistent signaling and aberrant proliferation and, in the *Arf-GFP* mouse, facilitates the accumulation of GFP-positive cells.

Some solid tumors that arose in $Arf^{GFP/GFP}$ mice and most of the lymphomas in $Arf^{+/GFP}$, Eμ-*Myc* transgenic animals produced sufficiently strong signals to allow their visualization by whole-body fluorescence imaging of live mice. Not all tumors exhibited such strong fluorescence at a macroscopic level, but when these were examined microscopically, we were invariably able to detect GFP-positive cells by immunohistochemistry. Many such tumors showed heterogeneous staining due to the presence of mixtures of normal and tumor cells. However, we cannot formally exclude the possibility that some tumor cells might segregate *Arf-GFP* alleles in the course of tumor progression. The *Arf* gene is closely flanked by two other tumor suppressors, *Ink4a* and *Ink4b*, within a segment of <100 kb in both the mouse and human genomes, and it is conceivable that selection against expression of either of the *Ink4* loci could result in deletions or epigenetic silencing of the *Arf* locus. Indeed, several examples exist in which *Arf* inactivation is followed by *Ink4a* loss of function, or vice versa, either during establishment of certain cultured cell lines (33) or in tumor development (4, 34–37).

Northern and immunoblotting assays have not documented *Arf* gene expression during mouse embryonic development (24). We recently used more sensitive RT-PCR analyses to repeat studies on early- and mid-gestation embryos and found that *Arf* transcripts are expressed in the yolk sac but are not readily detected in the embryo proper (L. Nilsson and F.Z., data not shown). After birth, low levels of *Arf* transcription were detected by RT-PCR in some organs of 4-month-old mice, and these remained essentially unchanged when reassayed in 15-month-old animals (24). In both young and old mice, the most prominent site of *Arf* expression was the testis; much lower levels were detected in spleen and lung, with barely detectable expression in kidney and brain. Although GFP expression could not be detected by using fluorescence microscopy of tissue sections taken from testes of adult $Arf^{GFP/GFP}$ mice, immunohistochemistry performed with antibodies to GFP identified positively staining cells in the testicular tubules that appeared to correspond to spermatogonia and/or very immature spermatocytes. We also observed foci of GFP-positive cells in thymus, lung, intestine, and brain and are currently attempting to characterize these cells in greater detail.

Although the roles that *Arf* may play in normal tissues largely remain a mystery, the *Arf-GFP* mouse should facilitate investigations of *Arf* temporal and spatial expression in various normal tissues. For example, *Arf* expression in the mouse eye is remarkably restricted. Normally, at birth, the retrolental vitreous contains delicate hyaloid vascular elements composed of endothelial and sparse perivascular cells. These vessels arise from the hyaloid artery at the optic disk, splay through the vitreous, and nourish the developing lens and pupillary membrane. Between postnatal days 6 and 10, this component of the hyaloid vasculature normally regresses, a process that does not occur in *Arf*-null mice in which excess perivascular cells accumulate (16). In normal animals, RT-PCR specifically identified *Arf* transcripts in the vitreous, but not in the optic cup or lens and only between postnatal days 1 and 5. A preliminary analysis of eyes from newborn $Arf^{+/GFP}$ mice has identified a few GFP-positive cells within the vitreous (data not shown), and we are now attempting to determine their lineage and how $p19^{Arf}$ prevents their excess accumulation. Regardless of their identity, the presence of fluorescent cells in the retrolental masses arising in $Arf^{GFP/GFP}$ mice now indicates that *Arf* plays a cell-autonomous role in their development.

Lymphoid cells from the spleen and bone marrow of $Arf^{+/GFP}$ mice bearing an Eμ-*Myc* transgene expressed GFP before any overt evidence of lymphoma existed. This corresponds to a time in the life history of the disease in which greatly increased lymphoid cell proliferation is offset by Arf- and p53-dependent apoptosis (18, 20, 29). Most GFP expression in lymphoid tissues of $Arf^{+/GFP}$, Eμ-*Myc* mice was confined to B220-positive B cells (28). In contrast, lymphoid tissues taken from control animals lacking the *Myc* transgene did not express GFP, underscoring the role of *Myc* as a potent *Arf* inducer and indicating, as well, that *Arf-GFP* expression in normal splenocytes or bone marrow cells (weakly positive by RT-PCR) was below the limit of detectability of the flow cytometric assay used. Despite the fact that B220-

positive cells in the spleen and bone marrow of *Arf*$^{+/GFP}$, Eμ-*Myc* transgenic mice expressed a significant number of green fluorescent cells, we could not detect splenic involvement in precancerous mice by whole-body imaging of live animals. However, lymph nodes from lymphomatous mice contained a sufficient concentration of GFP-positive cells to be imaged. Because *Arf* responds to many different oncogenic signals, including Ras, Abl, β-catenin, and others (38), and is inappropriately activated in animals lacking *Arf*-repressors such as Bmi-1 (39), breeding the *Arf-GFP* reporter strain to mice expressing these oncogenes or lacking such repressors, particularly in targeted somatic tissues, should similarly help to identify precancerous cells in other biologic settings.

We thank P. McKinnon and H. Russell for help with ES cells; S. Ragsdale for karyotyping; C. Nagy and G. Grosveld for ES injection and blastocyst implantation; E. Van de Kamp, W. den Besten, and J. Doherty for help constructing the targeting vector; G. Murti and K. Barnes for confocal microscopy; R. Ashmun and N. Carpino for flow cytometry; D. Bush and S. Portillo for immunohistochemical analyses; A. Martin for studies of the mouse eye; C. Hornsby and G. Assem for genotyping; and E. Vasquez for animal husbandry. This work was supported by National Institutes of Health Grants CA71907 (to M.F.R.), DK44158 and CA76379 (to J.L.C.), and T32-CA70089 (to R.T.W), Cancer Center Support Grant CA21765, National Research Service Award Grant F32-DK10154 (to T.A.B.), and American Lebanese Syrian Associated Charities of St. Jude Children's Research Hospital. C.J.S. is an investigator of the Howard Hughes Medical Institute.

1. Lowe, S. W. & Sherr, C. J. (2003) *Curr. Opin. Genet. Dev.* **13,** 77–83.
2. Serrano, M., Lee, H.-W., Chin, L., Cordon-Cardo, C., Beach, D. & DePinho, R. A. (1996) *Cell* **85,** 27–37.
3. Kamijo, T., Zindy, F., Roussel, M. F., Quelle, D. E., Downing, J. R., Ashmun, R. A., Grosveld, G. & Sherr, C. J. (1997) *Cell* **91,** 649–659.
4. Krimpenfort, P., Quon, K. C., Mooi, W. J., Loonstra, A. & Berns, A. (2001) *Nature* **413,** 83–86.
5. Sharpless, N. E., Bardeesy, N., Lee, K.-H., Carrasco, D., Castrillon, D. H., Aguirre, A. J., Wu, E. A., Horner, J. W. & DePinho, R. A. (2001) *Nature* **413,** 86–91.
6. Ruas, M. & Peters, G. (1998) *Biochim. Biophys. Acta* **1378,** F115–F177.
7. Esteller, M., Corn, P. G., Baylin, S. B. & Herman, J. G. (2001) *Cancer Res.* **61,** 3225–3229.
8. Quelle, D. E., Zindy, F., Ashmun, R. A. & Sherr, C. J. (1995) *Cell* **83,** 993–1000.
9. Zindy, F., Eischen, C. M., Randle, D. H., Kamijo, T., Cleveland, J. L., Sherr, C. J. & Roussel, M. F. (1998) *Genes Dev.* **12,** 2424–2433.
10. Palmero, I., Pantoja, C. & Serrano, M. (1998) *Nature* **395,** 125–126.
11. Weber, J. D., Jeffers, J. R., Rehg, J. E., Randle, D. H., Lozano, G., Roussel, M. F., Sherr, C. J. & Zambetti, G. P. (2000) *Genes Dev.* **14,** 2358–2365.
12. Carnero, A., Hudson, J. D., Price, C. M. & Beach, D. H. (2000) *Nat. Cell Biol.* **2,** 148–155.
13. Sugimoto, M., Kuo, M.-L., Roussel, M. F. & Sherr, C. J. (2003) *Mol. Cell* **11,** 415–424.
14. Kuo, M.-L., Duncavage, E. J., Mathew, R., den Besten, W., Pie, D., Naeve, D., Yamamoto, T., Cheng, C., Sherr, C. J. & Roussel, M. F. (2002) *Cancer Res.* **63,** 1046–1053.
15. Rocha, S., Campbell, K. J. & Perkins, N. D. (2003) *Mol. Cell* **12,** 15–25.
16. McKeller, R. N., Fowler, J. L., Cunningham, J. J., Warner, N., Smeyne, R. J., Zindy, F. & Skapek, S. X. (2002) *Proc. Natl. Acad. Sci. USA* **99,** 3848–3853.
17. McCarrick, J. W., Parnes, J. R., Seong, R. H., Solter, D. & Knowles, B. B. (1993) *Transgenic Res.* **2,** 183–190.
18. Eischen, C. M., Weber, J. D., Roussel, M. F., Sherr, C. J. & Cleveland, J. L. (1999) *Genes Dev.* **13,** 2658–2669.
19. Yang, M., Baranov, E., Jiang, P., Sun, F. X., Li, X. M., Li, L., Hasegawa, S., Bouvet, M., Al-Tuwaijri, M., Chrishima, T., *et al.* (2000) *Proc. Natl. Acad. Sci. USA* **97,** 1206–1211.
20. Schmitt, C. A., Fridman, J. S., Yang, M., Baranov, E., Hoffman, R. M. & Lowe, S. W. (2002) *Cancer Cell* **1,** 289–298.
21. Morgenstern, J. P. & Land, H. (1990) *Nucleic Acids Res.* **18,** 1068–1077.
22. Inoue, K., Wren, R., Rehg, J. E., Adachi, M., Cleveland, J. L., Roussel, M. F. & Sherr, C. J. (2000) *Genes Dev.* **14,** 1797–1809.
23. Zindy, F., Nilsson, L. M., Nguyen, L., Meunier, C., Smeyne, R. J., Rehg, J. E., Eberhart, C., Sherr, C. J. & Roussel, M. F. (2003) *Cancer Res.* **63,** 5420–5427.
24. Zindy, F., Quelle, D. E., Roussel, M. F. & Sherr, C. J. (1997) *Oncogene* **15,** 203–211.
25. Serrano, M., Lin, A. W., McCurrach, M. E., Beach, D. & Lowe, S. W. (1997) *Cell* **88,** 593–602.
26. Kamijo, T., Bodner, S., van de Kamp, E., Randle, D. H. & Sherr, C. J. (1999) *Cancer Res.* **59,** 2217–2222.
27. Kamijo, T., van de Kamp, E., Chong, M. J., Zindy, F., Diehl, A. J., Sherr, C. J. & McKinnon, P. (1999) *Cancer Res.* **59,** 2464–2469.
28. Adams, J. M., Harris, A. W., Pinkert, C. A., Corcoran, L. M., Alexander, W. S., Cory, S., Palmiter, R. D. & Brinster, R. L. (1985) *Nature* **318,** 533–538.
29. Schmitt, C. A., McCurrach, M. E., De Stanchina, E. & Lowe, S. W. (1999) *Genes Dev.* **13,** 2670–2677.
30. Jacobs, J. J. L., Scheijen, B., Vonchen, J.-W., Kieboom, K., Berns, A. & van Lohuizen, M. (1999) *Genes Dev.* **13,** 2678–2690.
31. Schmitt, C. A., Fridman, J. S., Yang, M., Lee, S., Baranov, E., Hoffman, R. M. & Lowe, S. W. (2002) *Cell* **109,** 335–346.
32. Zindy, F., den Besten, W., Chen, B., Rehg, J. E., Latres, E., Barbacid, M., Pollard, J. W., Sherr, C. J., Cohen, P. E. & Roussel, M. F. (2001) *Mol. Cell. Biol.* **21,** 3244–3255.
33. Randle, D. H., Zindy, F., Sherr, C. J. & Roussel, M. F. (2001) *Proc. Natl. Acad. Sci. USA* **98,** 9654–9659.
34. Bachoo, R. M., Maher, E. A., Ligon, K. L., Sharpless, N. E., Chan, S. S., You, M. J., Tang, Y., DeFrances, J., Stover, E., Weissleder, R., *et al.* (2002) *Cancer Cell* **1,** 269–277.
35. Bardeesy, N., Bastian, B. C., Hezel, A., Pinkel, D., DePinho, R. A. & Chin, L. (2001) *Mol. Cell. Biol.* **21,** 2144–2153.
36. You, M. J., Castrillon, D. H., Bastian, B. C., O'Hagan, R. C., Bosenberg, M. W., Parsons, R., Chin, L. & DePinho, R. A. (2002) *Proc. Natl. Acad. Sci. USA* **99,** 1455–1460.
37. Chin, L. (2003) *Nat. Rev. Cancer* **3,** 559–570.
38. Sherr, C. J. (2001) *Nat. Rev. Mol. Cell. Biol.* **2,** 731–737.
39. Jacobs, J. J. L., Kieboom, K., Marino, S., DePinho, R. A. & van Lohuizen, M. (1999) *Nature* **397,** 164–168.